Chemical Science

Accepted Manuscript

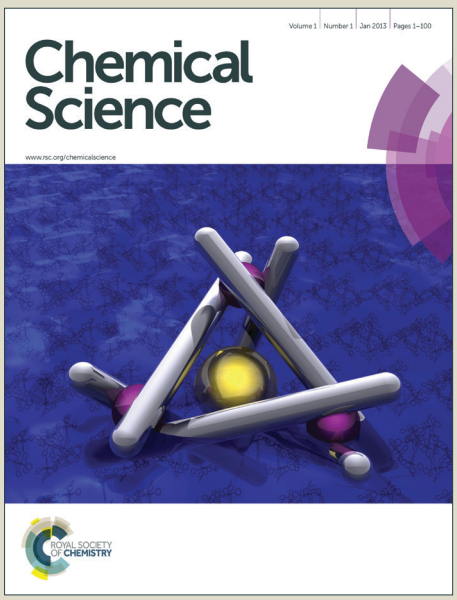

ROYAL SOCIETY OF CHEMISTRY

www.rsc.org/chemicalscience

Cite this: DOI: 10.1039/c0xx00000x

www.rsc.org/xxxxxx

ARTICLE TYPE

Engineering FRET Strategy to Achieve Ratiometric Two-Photon Fluorescence Response with Large Emission Shift and Its Application to Fluorescence Imaging

Lin Yuan,*[a] Fangping Jin,[a] Zebing Zeng,*[a] Chengbin Liu,[a] Shenglian Luo[a] and Jishan Wu[b]

Received (in XXX, XXX) Xth XXXXXXXXX 20XX, Accepted Xth XXXXXXXXX 20XX
DOI: 10.1039/b000000x

Two-photon excitation (TPE) probe-based fluorescence imaging has become one of the most attractive diagnostic techniques to investigate biomolecules and biological events in live cells and tissues. At the current stage most of the TPE-based sensing is reflected by fluorescence intensity changes. Nevertheless the mere altering of intensity could be facilely affected by ambient conditions. On the other hand, TPE probes based on intramolecular charge transfer (ICT) strategy could solve this problem to some extent with morphology change-induced emission shift. However their applications are yet constrained due to the inherent limitation of ICT, e.g. high degree of overlap of two emissions bands and shifts of the TPE maxima. To achieve desired TPE-based sensing and to circumvent the problems stated above, we adapted Förster resonance energy transfer (FRET) strategy to develop small molecule ratiometric TPE fluorescent probes. Our FRET-based ratiometric TPE fluorescent probe displays a remarkable emission shift (up to 125 nm) with two well-resolved emission bands. Hence the ratio of these two emission bands could enable measurement of fluorescence changes more characteristic and accurate, thus further benefited to imaging in live cells and deep tissues. To the best of our knowledge, the current reported probe *has the largest emission shift among all the small molecule ratiometric TPE fluorescent probes while the maximum TPE wavelength remains unchanged*. This work has provided a FRET approach to fabricate novel small molecule ratiometric TPE fluorescent probes that benefit the imaging in deep tissues.

Introduction

Small molecule fluorescent probes are intensely pursued in chemical biology research and medical diagnosis during the past thirty years because of their property, such as ability to improve analytical sensitivity, and in particular to offer capability for *in vivo* imaging studies with high spatiotemporal resolution.[1-4] Among the numerous molecular imaging techniques, two-photon excitation (TPE) probe-based fluorescence imaging stands out extraordinarily as result of its advantages in studying targeted biological molecules and biological events in live cells and deep tissues.[5,6] In addition to the advantages of conventional techniques such as superior sensitivity / selectivity, and non-invasiveness, TPE imaging is mostly prominent by featuring its deeper tissue penetration capability, substantially less photo-bleaching and photo-damage of the tissue, in virtue of the usage of low energy near infrared excitation. [7, 8]

High resolution TPE imaging is mostly attributed to the development of satisfying TPE fluorescent probes. Up to date, a large number of TPE fluorescent imaging probes have been developed that greatly contributed to biomedical research.[5, 6] However, most of the reported TPE sensing and imaging are relied on fluorescence intensity changes, which is easily influenced by many factors, including photo-bleaching, microenvironments (e.g. pH, polarity, temperature, and so forth), and local probe concentration. An effective strategy to overcome this shortcoming is the use of ratiometric fluorescent probes with concomitant changes of the intensities at dual-emission or dual-excitation bands.[9] Up to date, the ratiometric TPE fluorescent probes based on intramolecular charge transfer (ICT) strategy have been disclosed in literature,[10-16] where the background interference and false positive results were possibly weak. A few types of ICT probes exhibited extraordinary properties and were applied in cell or tissue imaging. Unfortunately, these ICT-based probes are usually haunted by certain undesirable photo-physical properties, which constrain the full potential for their applications. For instance, in many cases the ICT-based probes exhibit relatively broad emission spectra whereas their emission shift before and after interaction with the target bio-molecules is not prominent enough, thus resulting in a significant overlap between the shifted emission bands. This phenomenon severely limits the accurate measurement of the ratio of two emission bands. Furthermore, to choose a suitable TPE wavelength/source for these probes remains challenging as the maximum TPE wavelength is also remarkably fluctuated/shifted before and after reaction. Accordingly, we have to sacrifice one band of fluorescence brightness and irradiate at the excitation maxima of the other band; or we would equally sacrifice both bands of fluorescence brightness by irradiating at the iso-excitation point

to achieve two-photon ratiometric imaging. Therefore, given the weaknesses of ICT-based fluorescence probes, a brand new strategy to design and develop small-molecule ratiometric TPE probes with improved resolution of both emission bands and unchanged TPE wavelength for imaging in live cells and deep tissues is still highly demanded.

In view of the defects of ICT strategy that utilizes a single fluorophore to acquire ratiometric effects, we turned our attention to the Förster resonance energy transfer (FRET). FRET phenomenon involves the non-radiative transfer of excitation energy from an excited donor to a proximal ground-state acceptor.[17, 18] The advantage of FRET-based ratiometric probes over ICT probes lies in its superior emission shifts with fixed excitation wavelength.[17, 18] Surprisingly, although many FRET-based one-photon ratiometric fluorescent probes[17-29] and two-photon energy transfer cassettes[30-33] have been reported, to the best of our knowledge, there is no FRET-based small molecule ratiometric TPE fluorescent probe for deep-tissue imaging of specific biomolecules.

Herein we report the design of a simple yet efficient small molecule ratiometric TPE fluorescent probe based on FRET strategy by considering the following prerequisites: 1) large emission shift (> 80 nm) with two-well resolved emission bands before and after interaction with the analytes of interest; 2) a significant TPE cross-section with constant maximum TPE wavelength for a bright TPE imaging; 3) appreciable water solubility for cell/tissues permeability and staining; 4) a remarkable ratiometric response. Aiming at these targets, a TPE FRET cassette was constructed to develop a ratiometric fluorescent probe for hydrogen sulphide (H_2S). Notably, this probe demonstrated distinguished advantages of ratiometric fluorescent response with a large emission shift (up to 125 nm) and comparative fluorescence intensity. Moreover, the maximum TPE wavelength (donor moiety) of this probe barely shifted before and after interaction with H_2S. This probe was further applied for practical H_2S imaging in live cells and tissues by two-photon ratiometric mode. Hence in total, such FRET probe provides a new opportunity for biomedical researchers to explore accurate two-photon imaging using ratiometric TPE fluorescent probes with well-resolved emission spectra.

Results and Discussion

Design and Synthesis

Our design strategy of the ratiometric TPE fluorescent probe is to modulate TPE FRET efficiency in a two fluorophore cassette comprised of a well-known acedan (2-acetyl-6-dialkylaminonaphthalene)[34] moiety as a two-photon excitation donor and a H_2S-responsive anthocyanidin-analogue dye as an acceptor, linking by a rigid spacer. The two-photon fluorescence spectrum of acedan **2** matches well with the absorption spectrum of dye **6** (Figure S1a), but the gap of their emission bands is very large (130 nm) (Fig. S1a in ESI†). In addition, both **6** (Φ = 0.55) and **2** (Φ = 0.47) have substantial fluorescence quantum yields. These two factors are crucial for the effective FRET-based ratiometric fluorescent probes with superior emission shift and comparative fluorescence intensity. In the absence of H_2S, the acceptor shows a strong absorption in the acedan emission region and two-photon excitation of the donor chromophore should result in red acceptor emission by TPE-FRET. However, upon selective reaction with H_2S, the conjugated structure of acceptor is interrupted (Fig. S2 in ESI†), resulting in the decrease of the absorption of the acceptor in the donor emission region (Fig. S1b in ESI†). Thus FRET process is suppressed, and expected to green emission increase on excitation of the donor.

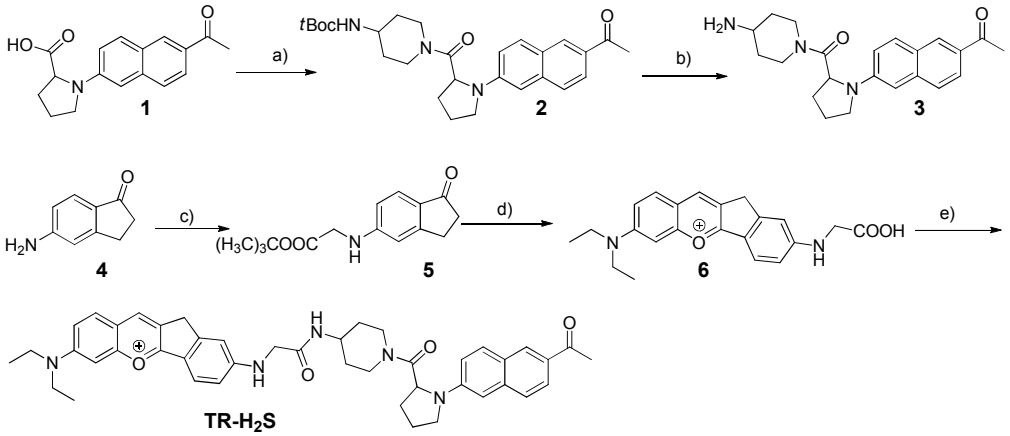

Scheme 1. Synthesis of probe **TR-H_2S**. Reaction conditions: a) 4-(*N*-Boc-amino)piperidine, EDC·HCl, HOBt; b) CF_3COOH/CH_2Cl_2; c) K_2CO_3, $BrCH_2CO_2C(CH_3)_3$; d) 4-(diethylamino)salicylaldehyde, $MeSO_3H$; e) **3,** EDC·HCl, HOBt. EDC·HCl= 1-ethyl-3-(3-dimethylaminopropyl) carbodiimide hydrochloride, HOBt = 1-hydroxybenzotriazole.

Probe **TR-H_2S** was facilely synthesized (Scheme 1) on the basis of the route shown in Scheme 1. The intermediate **3** was prepared in 78% yield by the coupling reaction between compound **1**[35] and 4-(*N*-Boc-amino)piperidine, followed by hydrolysis. Acceptor **6** was synthesized through a two-step reaction route. Reaction of compound **4** with *tert*-butyl bromoacetate under basic condition yielded compound **5**, which was further treated with 4-(diethylamino)salicylaldehyde in acidic condition to produce compound **6**. Finally, **TR-H_2S** was obtained by coupling **3** with **6** in 74% yield. All the new intermediates and resulting probe **TR-H_2S** were well characterized by ^{1}H NMR, ^{13}C NMR, HPLC-MS, and HRMS (ESI†).

Spectral properties

The absorption spectra, as well as two- and one-photon induced emission spectra of **TR-H_2S** in MeOH are illustrated in Fig. 1 and Fig. S3 (ESI†). Absorption spectra of **TR-H_2S** shows maximum characteristic of the donor at 378 nm and acceptor components at 578 nm (Fig. 1a). Irradiation of **TR-H_2S** at 378 (one-photon) or 760 nm (two-photon) resulted in emission mainly from the acceptor component with maximum at around 620 nm and a minor band at around 490 nm (Figure 1b and Fig. S3 in ESI†). This result is consistent with the FRET from the two-photon acedan donor to the anthocyanidin-analogue acceptor, indicating superior energy transfer efficiency (> 97%, by comparing the emission intensity of donor dye **2** and the residual emission of donor in FRET dyes). The high energy transfer efficiency was further reinforced by the excellent spectroscopic overlap between the normalized excitation and absorption spectra of **TR-H_2S** (Fig. S4 in ESI†).[36, 37] In addition, the fluorescence intensity of **TR-H_2S** has 2.6-fold brighter than the acceptor dye **6** as irradiation at 760 nm (Fig. 1b).

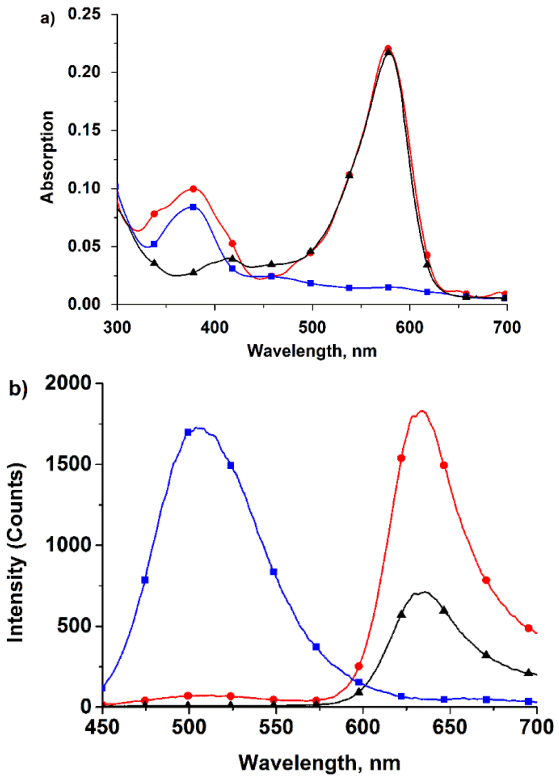

Fig. 1. Absorption (a) and two-photon (λ_{ex} = 760 nm) induced emission spectra (b) of **TR-H_2S** (●), **2** (■), and **6** (▲) at 25 °C in MeOH. Emission at around 500 nm is quenched (>97%) upon excitation of **TR-H_2S** at 760 nm compared to excitation of **2** at 760 nm.

We then investigated the spectral response of probe to H_2S. As expected, once H_2S was added to the probe solution, the fluorescence tint changes from crimson to green (inset in Fig. 2a), while the emission wavelength was measured to shift from 620 nm to 497 nm upon excitation at 378 nm. This is because the nucleophilic attack of H_2S towards the benzopyrylium moiety of the acceptor interrupts its π-conjugation, thereby leading to the decrease of acceptor absorption (Fig. 2b) as well as descending of FRET efficiency.[38] To further examine the H_2S-based quenching mechanism, HPLC-MS was used to clarify the process of the reaction between **6** and Na_2S. The HPLC chromatogram of **6** was shown in Fig. S2a (ESI†). After incubation with Na_2S for 1 min (Fig. S2b in ESI†), a new peak with longer retention time was observed, which was attributed to form a neutral **6**-SH adduct deduced through mass spectra (Fig. S2c in ESI†). The proposed neutral **6**-SH product was further supported by ^{1}H NMR titration studies (Fig. S2d in ESI†), which showed that almost all aromatic proton signals shifted to up-field upon addition of Na_2S to the solution of compound **6**.

We further investigated the concentration dependent fluorescence response of probe **TR-H_2S** to H_2S under two-photon (760 nm) excitation model. As shown in Fig. 2c, upon addition of Na_2S (0–200 μM), the emission intensity at 625 nm gradually decreased with the simultaneous appearance of a new blue emission peak centred at 500 nm. Meanwhile a clear iso-emission point was observed at 588 nm. Essentially, the intensity ratio (I_{500}/I_{625}) lineally increased when the concentration of Na_2S changed from 1 to 80 μM whereas the detection limit was determined to be 0.3 μM based on signal-to-noise ratio (S/N) = 3 (Fig. S5 in ESI†), and the highest intensity ratio (I_{500}/I_{625}) change with a 796-fold enhancement was achieved by addition of 200 μM Na_2S. Impressively, the shift of two emission bands is very large (emission shift: $\Delta\lambda$ = 125 nm) with comparative fluorescence intensity, thus generating two well-resolved emission bands. This resolution is in favour of the accurate two-photon imaging owing to the huge *ratiometric value* induced by the remarkable intensities of the two emission bands. This mega-emission shift is distinctively larger than through-bond energy transfer (TBET)-based ratiometric TPE probes.[39] *To the best of our knowledge, it has the largest emission shift for small molecule ratiometric TPE fluorescent probes.* The observation validates our design concept that FRET is an efficient strategy to develop ratiometric TPE fluorescent probe with large emission shift and well resolved emission bands. It is noteworthy that the maximum two-photon excitation wavelength of the donor moieties at 760 nm remains fixed (Fig. 2d), which is significantly superior than ratiometric TPE probes related to ICT, thus FRET probe is more suitable for accurate two-photon imaging. Different photobleaching rates of donor and acceptor of FRET-based probes can affect the donor-acceptor ratio, and thus would bias ratiometric measurements. Thus, we measure the fluorescence intensity of acedan **2** and anthocyanidin **6** after exposure to light. As shown in Fig. S6a (ESI†), the relative fluorescence intensity of both **2** and **6** gradually decreased after long time exposure to UV light (80 W, 365 nm). However, the relative fluorescence intensity of both **2** and **6** almost unchanged exposure to femtosecond laser (80 W, 760 nm) (Fig. S6b in ESI†). *This is because photobleaching of the dyes are less likely to occur within the restricted excitation volume characteristic of two-photon excitation.*[40] As expected, the emission ratio of probe **TR-H_2S** almost unchanged after exposure 760 nm (80 W) for 40 min (Fig. S6c in ESI†). Above results suggest that FRET-based ratiometric TPE fluorescent probes is less affected by photobleaching, thereby more suitable for bioimaging application.

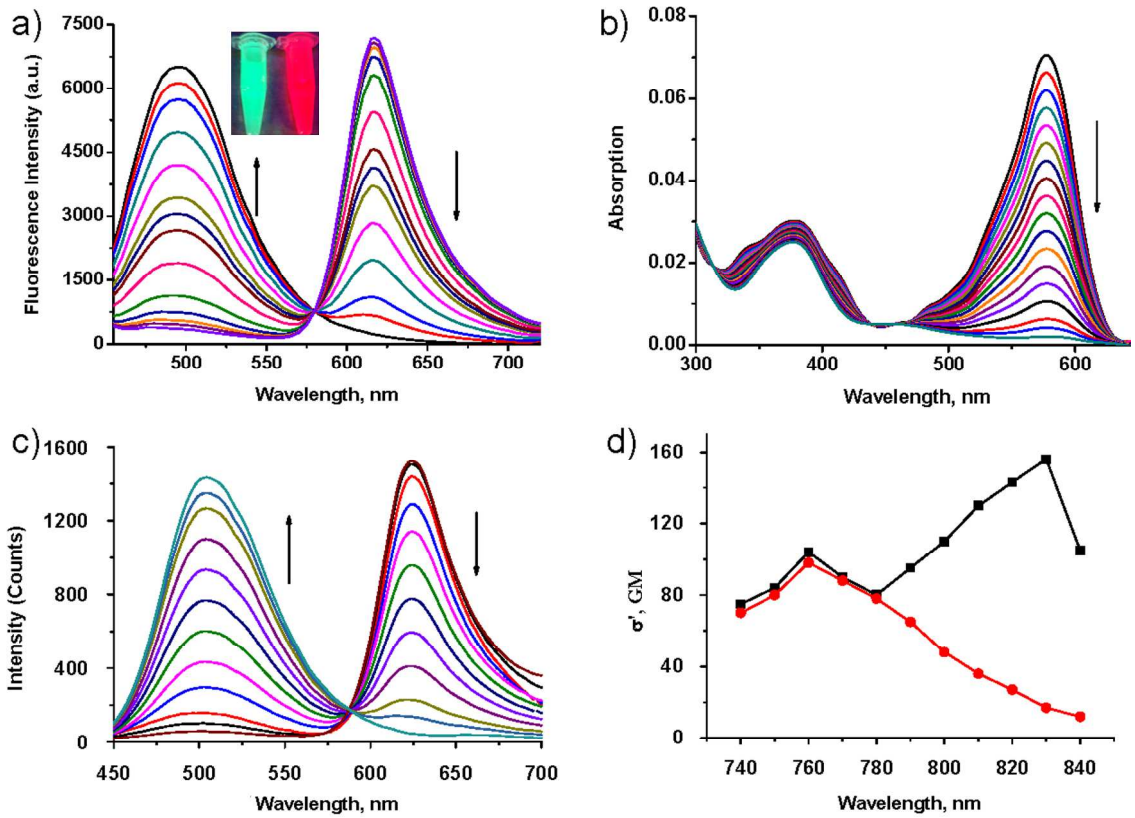

Fig. 2. Spectra properties of **TR-H_2S** (5 μM) upon titration of H_2S (Na_2S, 0-200 μM) in a PBS (pH = 7.4, 2% DMSO, 1 mg/mL HSA): (a) one-photon excitation emission spectra (λ_{ex} = 378 nm); (b) absorption spectra; (c) two-photon excitation emission spectra (λ_{ex} = 760 nm). (d) Two-photon absorption cross section of **TR-H_2S** in the absence (■) and presence of H_2S (●) (200 μM).

The ratio change of probe **TR-H_2S** to H_2S was very fast and reached a plateau within 30 seconds (Fig. S7 in ESI†), suggesting that **TR-H_2S** favors to real-time tracking of H_2S concentration changes. Moreover, **TR-H_2S** can respond to H_2S on a biologically relevant pH level (Fig. S8 in ESI†). Thus, we further evaluated the specific nature of this probe by co-incubation with relevant reactive sulfur (RSS), oxygen (ROS), nitrogen species (RNS), along with some cations and anions. As shown in Fig. 3, only H_2S could lead to pronounced enhancement of fluorescence intensity ratios (I_{500}/I_{625}). Other biologically relevant RSS (GSH, cysteine, SO_4^{2-}, $S_2O_3^-$, SCN^-), RNS (NO_2^-, NO_3^-, NO, $NH_3{\cdot}H_2O$), ROS (*t*-BuOOH, H_2O_2, $O_2^{\cdot-}$, $HO^{\cdot}$, HOCl), amino acids without thiol groups (Lys, Glu), metal ions and anions (Ca^{2+}, K^+, Na^+, Zn^{2+}, Mg^{2+}, N_3^-, CN^-) showed minimum interference (Fig. 3). The excellent selectivity enable **TR-H_2S** suitably detect H_2S in rather complex biological environment. The high selectivity of **TR-H_2S f**or H_2S over other biological thiols can be rationalized on the basis of different p*Ka* values of thiols and electrostatic repulsion. It has been reported that H_2S in aqueous solution has a p*Ka* value lower than 6.9 whereas other biothiols have higher p*K*a values (e.g. Cys, 8.30; GSH, 9.20).[41] Thus, H_2S is a better nucleophile than other biothiols under physiological media. In addition, both probe **TR-H_2S** and Cys or GSH have a cationic group, which will prevent their effective collisions (Fig. S9 in ESI†). This high selectivity of positive dye **TR-H_2S** for H_2S over other biothiols is in good agreement with previous reports.[38, 42]

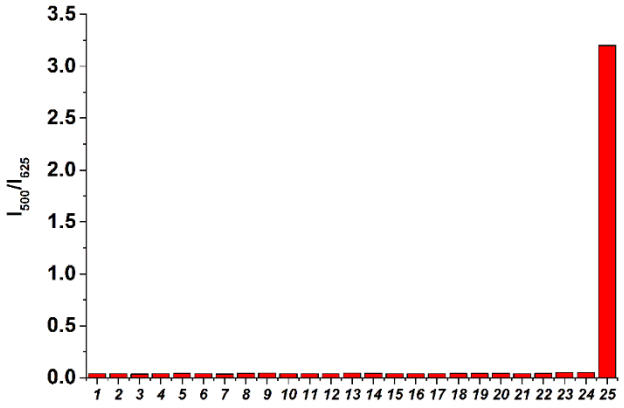

Fig. 3. Fluorescence intensity ratios (I_{500}/I_{625}) responses of probe **TR-H_2S** (2 μM) to representative species in PBS buffer (pH = 7.4, 2% DMSO, 1 mg/mL HSA). (1) Free, (2) *t*BuOOH (200 μM), (3) NO (200 μM), (4) (5) H_2O_2 (200 μM), (6) KO_2, (200 μM), (7) Lys (200 μM), (8) HOCl (100 μM), (9) $NH_3{\cdot}H_2O$ (200 μM), (10) $HO{\cdot}$(200 μM), (11) NO_2^- (200 μM), (12) NO_3^- (200 μM), (13) Glu (200 μM), (14) N_3^- (200 μM), (15) CN^-(200 μM), (16) K^+ (5 mM), (17) Na^+ (5 mM), (18) Ca^{2+} (1 mM), (19) Zn^{2+} (1 mM), (20) Mg^{2+} (500 μM), (21) $S_2O_3^{2-}$ (200 μM); (22) SCN^- (100 μM); (22) SO_4^{2-} (500 μM); (23) Cys (1 mM), (24) GSH (5 mM), (25) H_2S (100 μM).

The properties of probe **TR-H_2S** and some previously published small-molecular ratiometric fluorescent H_2S probes based on ICT,[10, 38, 42-49] FRET[50, 51] and excited state intramolecular proton transfer (ESIPT)[52-55] mechanism are summarized in Table S1, in which all the probes have moderate

selectivity for H_2S over other biothiols. The fluorescent detection limit of probe **TR-H_2S** was 0.3 μM (Table S1, ESI†), which is comparable with most ratiometric H_2S probes. However, probe **TR-H_2S** collectively displays several unique advantages, such as its large emission shift (125 nm), unchanged maximum low energy TPE wavelength (760 nm) and both emission bands located at long wavelength region (500-630 nm).

Cell and tissue imaging

Overall, probe **TR-H_2S** displays high selectivity and fast response towards H_2S at physiological pH accompanying with two well-resolved emission bands. In addition, probe **TR-H_2S** also displays negligible toxicity through MTT assay (Fig. S10 in ESI†). The above results suggest that **TR-H_2S** is promising for applications in biological systems. We then tested the capability of probe **TR-H_2S** for ratiometric imaging of H_2S in living cells and tissue. We first investigated whether this probe can be applied to fluorescence imaging of deep tissues before and after interaction with the H_2S. As shown in Fig. S11-12 (ESI†), rat liver tissue samples incubated with only probe **TR-H_2S** (Fig. S11) or incubated with **TR-H_2S** for 30 minutes and then further incubated with H_2S (Fig. S12) showed a strong red or green fluorescence at 90-180 μM by TPM, respectively. Therefore, **TR-H_2S** possess good tissue penetration, and could be useful as imaging of dual-colour deep tissue.

Liver slices incubated with **TR-H_2S** displayed a strong fluorescence at red channel (Fig. 4b) and slight fluorescence at green channel (Fig. 4a). However, in the presence of H_2S, a partial quenching of fluorescence at red channel (Fig. 4e) and a remarkable increase of fluorescence at the green channel (Fig. 4d) was observed. Thus, the ratio data significantly increased (Fig. 4c, 4f and Fig. S13 in ESI†), which was obtained using commercial software. A similar phenomenon is also observed for cell imaging (Fig. S14 in ESI†). These experiments indicated that probe **TR-H_2S** can provide ratiometric TPE detection of H_2S at cell and tissue level with less cross talk between dual emission channels. Therefore, probe **TR-H_2S** has a potential to serve as an efficient molecular probe for the study biological processes involving H_2S within live cells and tissue.

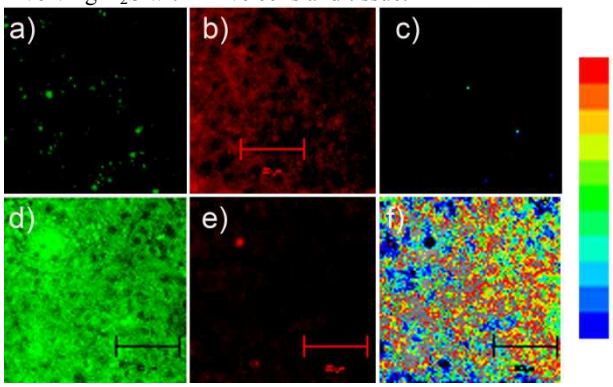

Fig. 4. Two photon imaging of rat liver slice upon excitation at 780 nm with femtosecond pulses: a-c) Liver slice incubated with **TR-H_2S** (5 μM) for 30 min, emission measured at 471-560 nm (a) and 591-704 nm (b); (c) the ratio of a and b; d-f) Liver slice incubated with **TR-H_2S** (5 μM) for 30 min and then further incubated with H_2S (100 μM) for 30 min, emission measured at 471-560 nm (d) and 591-704 nm (e); (f) the ratio of d and e. Scale bars: 100 μm

Conclusions

In summary, we provided a FRET approach to fabricate novel small molecule ratiometric TPE fluorescent probe benefiting imaging in deep tissues. To prove the concept, a ratiometric TPE fluorescent probe - **TR-H_2S** - for H_2S monitoring was developed, which displayed a large emission shift (125 nm), two-well resolved emission bands and fixed maximum TPE wavelength (donor moieties). Thus **TR-H_2S** can achieve accurate measurement of two band fluorescence with less cross talk and have realized H_2S detection in live cells and tissues in two-photon ratiometric mode. This strategy provides a new opportunity for biomedical researchers to pursue two-photon ratiometric fluorescent probes with well-resolved emission spectra. Future work, such as two-or more energy donor assisted enhanced two-photon excited fluorescence for ratiometric imaging is in progress.

Acknowledgments

This work was financially supported by NSFC (21302050), the Hunan Provincial Natural Science Foundation of China (14JJ2047), the Fundamental Research Funds for the Central Universities, and the Startup Fund (531109020043) from Hunan University.

Notes and references

[a] *State Key Laboratory of Chemo/Biosensing and Chemometrics, College of Chemistry and Chemical Engineering, Hunan University, Changsha 410082 (PR China); E-mail: lyuan@hnu.edu.cn; zbzeng@hnu.edu.cn*
[b] *Department of Chemistry, National University of Singapore, 3 Science Drive 3, 117543, Singapore*

† Electronic Supplementary Information (ESI) available: [Synthetic procedures and characterization data; additional spectroscopic data]. See DOI: 10.1039/b000000x/

1. H. Kobayashi, M. Ogawa, R. Alford, P. L. Choyke and Y. Urano, *Chem. Rev.*, 2010, **110**, 2620-2640.
2. K. P. Carter, A. M. Young and A. E. Palmer, *Chem. Rev.*, 2014, **114**, 4564-4601.
3. J. Chan, S. C. Dodani and C. J. Chang, *Nat. Chem.*, 2012, **4**, 973-984.
4. X. Li, X. Gao, W. Shi and H. Ma, *Chem. Rev.*, 2014, **114**, 590-659.
5. D. Kim, H. G. Ryu and K. H. Ahn, *Org. Biomol. Chem.*, 2014, **12**, 4550-4566.
6. S. Yao and K. D. Belfield, *Eur. J. Org. Chem.*, 2012, 3199-3217.
7. F. Helmchen and W. Denk, *Nat. Methods*, 2005, **2**, 932-940.
8. W. R. Zipfel, R. M. Williams and W. W. Webb, *Nat. Biotechnology*, 2003, **21**, 1369-1377.
9. J. S. K. Min Hee Lee and J. L. Sessler, *Chem. Soc. Rev.*, 2014, DOI: 10.1039/C1034CS00280F.
10. S. K. Bae, C. H. Heo, D. J. Choi, D. Sen, E. H. Joe, B. R. Cho and H. M. Kim, *J. Am. Chem. Soc.*, 2013, **135**, 9915-9923.
11. Q. Q. Wu, Z. F. Xiao, X. J. Du and Q. H. Song, *Chem.-Asian J.*, 2013, **8**, 2564-2568.
12. C. Chung, D. Srikun, C. S. Lim, C. J. Chang and B. R. Cho, *Chem. Commun.*, 2011, **47**, 9618-9620.
13. H. J. Kim, C. H. Heo and H. M. Kim, *J. Am. Chem. Soc.*, 2013, **135**, 17969-17977.
14. S. K. Bae, C. H. Heo, D. J. Choi, D. Sen, E. H. Joe, B. R. Cho and H. M. Kim, *J. Am. Chem. Soc.*, 2013, **135**, 9915-9923.

15. F. Liu, T. Wu, J. F. Cao, S. Cui, Z. G. Yang, X. X. Qiang, S. G. Sun, F. L. Song, J. L. Fan, J. Y. Wang and X. J. Peng, *Chem.-Eur. J.*, 2013, **19**, 1548-1553.
16. S. Sumalekshmy, M. M. Henary, N. Siegel, P. V. Lawson, Y. Wu, K. Schmidt, J. L. Bredas, J. W. Perry and C. J. Fahrni, *J. Am. Chem. Soc.*, 2007, **129**, 11888-11889.
17. J. Fan, M. Hu, P. Zhan and X. Peng, *Chem. Soc. Rev.*, 2013, **42**, 29-43.
18. L. Yuan, W. Lin, K. Zheng and S. Zhu, *Acc. Chem. Res.*, 2013, **46**, 1462-1473.
19. W. Xuan, Y. Cao, J. Zhou and W. Wang, *Chem. Commun.*, 2013, **49**, 10474-10476.
20. H. Yu, Y. Xiao, H. Guo and X. Qian, *Chem. -Eur. J.*, 2011, **17**, 3179-3191.
21. X. Zhang, Y. Xiao and X. Qian, *Angew. Chem.-Int. Ed.*, 2008, **47**, 8025-8029.
22. A. E. Albers, V. S. Okreglak and C. J. Chang, *J. Am. Chem. Soc.*, 2006, **128**, 9640-9641.
23. L. Yuan and Q. P. Zuo, *Chem.-Asian J.*, 2014, **9**, 1544-1549.
24. Y. X. Wu, X. B. Zhang, J. B. Li, C. C. Zhang, H. Liang, G. J. Mao, L. Y. Zhou, W. Tan and R. Q. Yu, *Anal. Chem.*, 2014, **86**, 10389-10396.
25. D. H. Ma, D. Kim, T. Akisawa, K. H. Lee, K. T. Kim and K. H. Ahn, *Chem.-Asian J.*, 2014, doi: 10.1002/asia.201403073.
26. Y. Chen, C. Zhu, J. Cen, J. Li, W. He, Y. Jiao and Z. Guo, *Chem. Commun.*, 2013, **49**, 7632-7634.
27. Y. Kurishita, T. Kohira, A. Ojida and I. Hamachi, *J. Am. Chem. Soc.*, 2010, **132**, 13290-13299.
28. R. Guliyev, A. Coskun and E. U. Akkaya, *J. Am. Chem. Soc.*, 2009, **131**, 9007-9013.
29. J. R. Cox, P. Muller and T. M. Swager, *J. Am. Chem. Soc.*, 2011, **133**, 12910-12913.
30. L. Liu, M. Shao, X. Dong, X. Yu, Z. Liu, Z. He and Q. Wang, *Anal. Chem.*, 2008, **80**, 7735-7741.
31. D. W. Brousmiche, J. M. Serin, J. M. Frechet, G. S. He, T. C. Lin, S. J. Chung and P. N. Prasad, *J. Am. Chem. Soc.*, 2003, **125**, 1448-1449.
32. Roussakis, J. A. Spencer, C. P. Lin and S. A. Vinogradov, *Anal. Chem.*, 2014, **86**, 5937-5945.
33. L. Liu, G. Wei, Z. Liu, Z. He, S. Xiao and Q. Wang, *Bioconjugate Chem.*, 2008, **19**, 574-579.
34. E. W. Seo, J. H. Han, C. H. Heo, J. H. Shin, H. M. Kim and B. R. Cho, *Chem.-Eur. J.*, 2012, **18**, 12388-12394.
35. M. Y. Kang, C. S. Lim, H. S. Kim, E. W. Seo, H. M. Kim, O. Kwon and B. R. Cho, *Chem.-Eur. J.*, 2012, **18**, 1953-1960.
36. S. L. Gilat, A. Adronov and J. M. J. Frechet, *Angew. Chem. Int. Et.*, 1999, **38**, 1422-1427.
37. S. P. Balashov, E. S. Imasheva, J. M. Wang and J. K. Lanyi, *Biophys. J.*, 2008, **95**, 2402-2414.
38. J. Liu, Y. Q. Sun, J. Zhang, T. Yang, J. Cao, L. Zhang and W. Guo, *Chem.-Eur. J.*, 2013, **19**, 4717-4722.
39. L. Zhou, X. Zhang, Q. Wang, Y. Lv, G. Mao, A. Luo, Y. Wu, Y. Wu, J. Zhang and W. Tan, *J. Am. Chem. Soc.* 2014, **136**, 9838-9841.
40. P. Schwille, U. Haupts, S. Maiti and W. W. Webb, *Biophys. J.*, 1999, **77**, 2251-2265.
41. H. Peng, W. Chen, Y. Cheng, L. Hakuna, R. Strongin and B. Wang, *Sensors*, 2012, **12**, 15907-15946.
42. Y. Chen, C. Zhu, Z. Yang, J. Chen, Y. He, Y. Jiao, W. He, L. Qiu, J. Cen and Z. Guo, *Angew. Chem.-Int. Ed.*, 2013, **52**, 1688-1691.
43. F. Yu, P. Li, P. Song, B. Wang, J. Zhao and K. Han, *Chem. Commun.*, 2012, **48**, 2852-2854.
44. X. L. Liu, X. J. Du, C. G. Dai and Q. H. Song, *J. Org. Chem.*, 2014, **79**, 9481-9489.
45. M. Y. Wu, K. Li, J. T. Hou, Z. Huang and X. Q. Yu, *Org. Biomol. Chem.*, 2012, **10**, 8342-8347.
46. L. Zhang, W. Q. Meng, L. Lu, Y. S. Xue, C. Li, F. Zou, Y. Liu and J. Zhao, *Sci. Rep.*, 2014, **4**, 5870.
47. J. S. Xu Wang, W. Zhang, X. Ma, J. Lv and B. Tang, *Chem. Sci.*, 2013, **4**, 2551-2556.
48. L. Zhang, S. Li, M. Hong, Y. Q. Xu, S. S. Wang, Y. Liu, Y. Qian and J. Zhao, *Org. Biomol. Chem.*, 2014, **12**, 5115-5125.
49. Q. Q. Wan, Y. C. Song, Z. Li, X. H. Gao and H. M. Ma, *Chem. Commun.*, 2013, **49**, 502-504.
50. L. Yuan and Q. P. Zuo, *Chem. Asian. J.*, 2014, **9**, 1544-1549.
51. L. Wei, L. Yi, F. Song, C. Wei, B. F. Wang and Z. Xi, *Sci. Rep.*, 2014, **4**, 4521.
52. Y. Jiang, Q. Wu and X. Chang, *Talanta*, 2014, **121**, 122-126.
53. Q. Huang, X. F. Yang and H. Li, *Dyes. Pigment.*, 2013, **99**, 871-877.
54. Z. Xu, L. Xu, J. Zhou, Y. Xu, W. Zhu and X. Qian, *Chem. Commun.*, 2012, **48**, 10871-10873.
55. S. Goswami, A. Manna, M. Mondal and D. Sarkar, *Rsc. Adv.*, 2014, **4**, 62639-62643.

Cite this: DOI: 10.1039/c0xx00000x

www.rsc.org/xxxxxx

ARTICLE TYPE

TOC

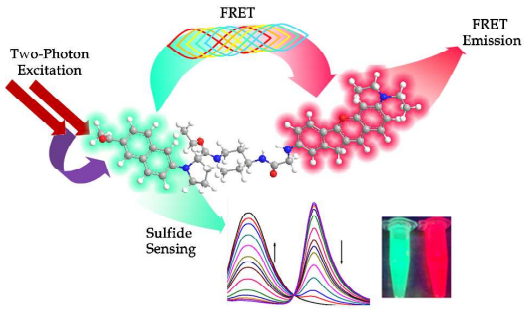

A FRET strategy was applied to develop ratiometric two-photon fluorescent probe with large emission shift for imaging in cell and tissue.